

The molecular relaxation mechanisms in cork as studied by thermally stimulated discharge currents

J. F. MANO, N. T. CORREIA, J. J. MOURA RAMOS*, B. SARAMAGO*‡
Centro de Química-Física Molecular, and ‡ Centro de Química Estrutural, Complexo I, IST, Av. Rovisco Pais, 1096 Lisboa Codex, Portugal

The dielectric relaxation mechanisms present in cork have been investigated in the temperature range -100 to 100 °C using the technique of thermally stimulated discharge currents. A relaxation mechanism was detected which showed a compensation behaviour as observed for the α -relaxation (or glass transition relaxation) of synthetic polymers and which lead us to attribute to cork a glass transition-like temperature of 18 °C. One lower temperature mechanism was also observed, with low activation enthalpy and entropy, which is presumably originated by local motions (internal rotations) of polar molecular groups. An upper T_g relaxation of higher intensity was also detected which was attributed to large-scale non-cooperative motions of polymeric segments.

1. Introduction

Cork is a natural material whose remarkable properties have been exploited by man since ancient times. The cork tissue is the bark of an oak which grows in the Mediterranean countries. In Portugal, cork has great economical importance with 30% of the total value of portuguese exports being cork-based.

The most widespread use of cork has been in the production of stoppers for wine bottles. The Romans, who cared about good wine, used cork to seal their bottles. It is, in fact, known that a perfect sealing is essential to keep the quality of the wine. Owing to its mechanical behaviour and chemical stability, cork is an excellent material to perform this role. The cellular structure of cork makes it, on the other hand, a very good thermal and acoustic insulator. It is used to provide insulation in refrigerators and houses through the lining of walls and floors. The cellular structure of cork also explains its ability to absorb energy which is used in packaging and manufacturing of shoe soles.

The description of the structure of cork dates back to the seventeenth century when Robert Hooke first examined cork under the microscope. In the 1950s Natividade [1] confirmed that cork is a cellular material with closed prismatic cells packed in columns parallel to the radial direction of the tree. The cell dimensions depend on the season in which they were generated. Spring cells are 30 – 40 μm long with thin walls and the height of the autumn cells decreases to 10 – 15 μm with thicker walls. Besides the radial direction, two other directions are defined in order to describe the anisotropy of this material: the axial direction parallel to the axis of the tree and the tan-

gential direction perpendicular to the other two. Fig. 1 shows cork sections perpendicular to the three main directions observed with a scanning electron microscope. Several defects disturb the regular distribution of cells. Among these, cork always exhibits lenticular channels along the radial direction which appear as randomly distributed pores in the sections perpendicular to this direction. The size and density of the pores determine the quality of the cork.

Chemically, cork consists of suberin (30%), lignin (30%), celluloses and hemicelluloses (20%), extractables (waxes and tannins) (15%) and ash (5%) [2]. The cellular walls are made up of a lignin- and cellulose-rich middle lamella and a thicker secondary layer with alternating lamellae of suberin and waxes [3]. The cells are closed units which are filled with a gaseous mixture similar to air.

Much of the work which has been done on cork deals with physical aspects of cork research, such as morphology and mechanical properties [4–7]. Recently, studies on the surface properties of cork were reported [8, 9]. These studies are important to understand the adhesion mechanisms involving the surface of cork which is largely used in industry in the form of cork composites.

Another important application of cork is as an electric insulator (it is a dielectric material). Nevertheless, the study of the dielectric properties of cork was never undertaken and the aim of this work was precisely to carry out a systematic study of the behaviour of cork under the presence of electric static fields. The technique used was that of thermally stimulated discharge currents (TSDC) with the hope that the results

* Authors to whom all correspondence should be addressed.

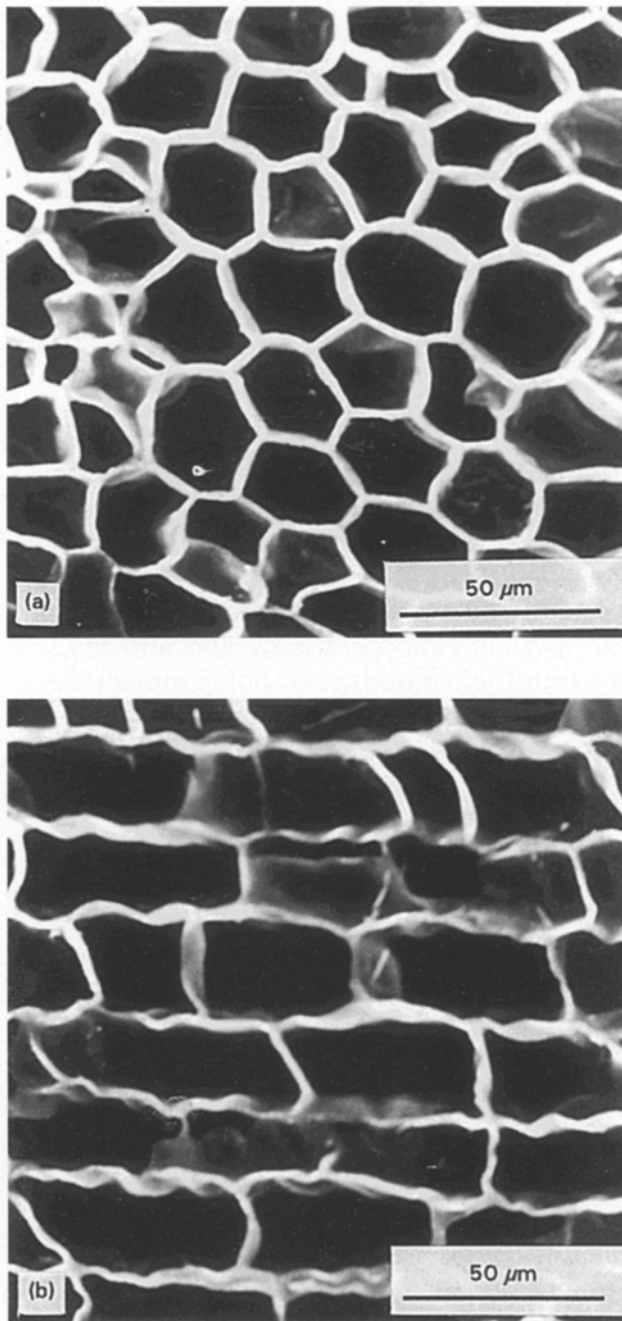


Figure 1 Scanning electron micrographs of sections perpendicular to (a) the radial direction and (b) the axial or tangential direction.

obtained would improve knowledge about the dipolar motions which are activated in cork by the presence of an electric field. This is a pioneer work, because no other study of cork using the TSDC technique has been previously published. In the more general context of natural materials, TSDC studies are also very scarce, a very recent study on bone having only just been reported [10].

2. Experimental procedure

Thermally stimulated current experiments were carried out with a TSC/RMA Spectrometer (Solomat Instruments, Stamford, CT) covering the temperature range -170 to 400°C . A Faraday cage shields the sample and prior to the experiments the sample is

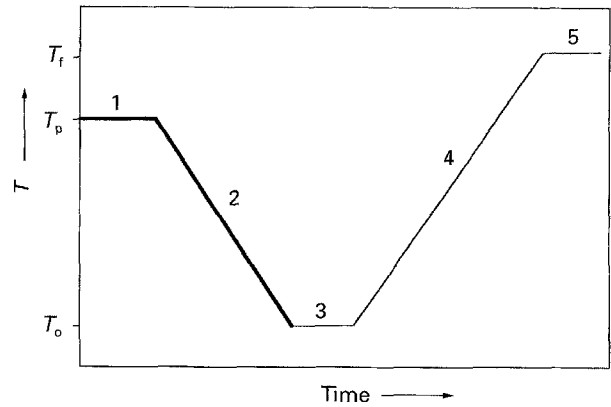


Figure 2 Schematic representation of a TSDC global experiment. The numbers refer to the different steps of the experiment. The electric field is applied in steps 1 and 2 (thicker lines). The polarization current is measured during the constant rate heating process – step 4.

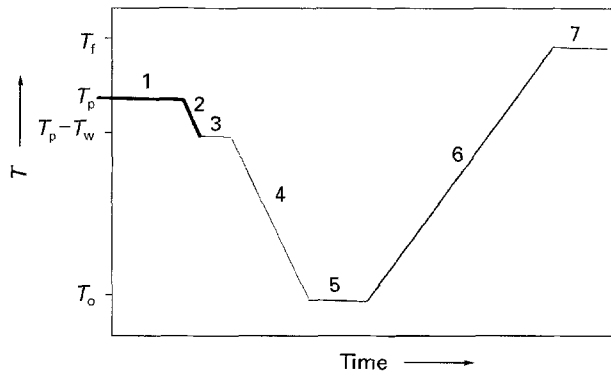


Figure 3 Schematic representation of a thermal windowing experiment. The electric field is applied in steps 1 (isothermal polarization at T_p) and 2 (freezing of the components of the polarization between T_p and $T_p - T_w$). The depolarization current is measured during the constant rate heating process – step 6.

evacuated to 10^{-4} mbar and flushed three times with 1.1 bar high-purity helium. In order to analyse the different regions of the TSDC spectrum, different methods of polarizing the sample were used, namely the so-called TSDC global experiments and the thermal windowing (or cleaning) experiments [11, 12]. In a TSDC global experiment (see Fig. 2) the electric field is applied in a wide temperature range from T_p (the polarization temperature) to a lower temperature, T_0 . Under these conditions, the sample is polarized and a complex pattern of polarization mechanisms is activated between T_p and T_0 . The sample is then heated at a constant rate from T_0 to a temperature T_f higher than T_p and the depolarization current intensity is measured as a function of temperature.

In a thermal windowing experiment, on the other hand (see Fig. 3), the electric field is applied in a narrow temperature range from T_p to a lower temperature T_w (in the present work $T_p - T_w = 3^{\circ}\text{C}$). At T_w the voltage is turned off and the sample is cooled to T_0 and then heated at constant rate to T_f . In this heating process the depolarization current intensity is measured as a function of temperature. In a thermal windowing experiment only a narrow range of the complex polarization mechanisms is allowed to be polarized and thus the technique enables the single or

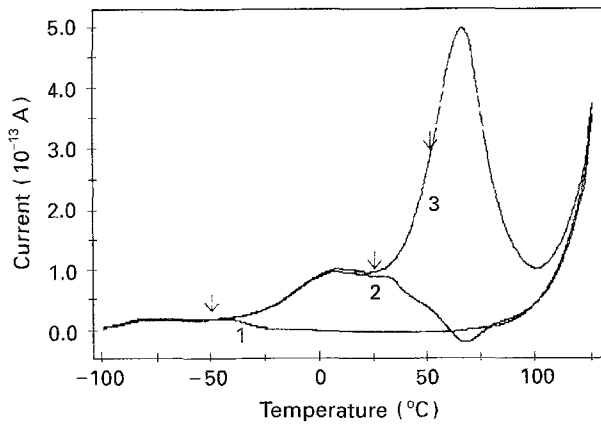


Figure 4 TSDC global spectra obtained at different polarization temperatures: 1, $T_p = -50^\circ\text{C}$; 2, $T_p = 25^\circ\text{C}$; 3, $T_p = 50^\circ\text{C}$. For these experiments $T_0 = -100^\circ\text{C}$ and $T_f = 125^\circ\text{C}$.

individual components of the complex relaxation spectrum to be isolated.

First-quality cork is determined by low porosity, and all our measurements were carried out on such a material. After boiling in water for 1 h and air drying, the cork was cut with a razor blade into rectangular slices $\sim 7 \times 6 \times 0.6$ mm perpendicular to the tangential direction (see Section 1). This section was chosen because it offers larger surface areas free of defects. The moisture content of cork upon equilibration with the laboratory atmosphere varies between 5% and 7%. Different cork samples were studied and the results showed an extremely good reproducibility. Before each experiment, the sample was annealed at 90°C for 10 min.

3. Results and discussion

Different TSDC global experiments were carried out in the temperature range -100 to 100°C in order to distinguish the different regions of the TSDC spectrum. The results of some of these experiments are shown in Fig. 4. It can be observed that the intensity of the discharge current is an increasing function of the temperature up to a value near T_p (the polarization temperature is indicated by an arrow for each experiment in Fig. 4). Several regions can be distinguished in the global TSDC spectrum (refer, for example, to curve 3 in Fig. 4): (a) from -100 to -50°C where the intensity of the discharge current is small and remains nearly constant; (b) from -50 to 5°C where the discharge current increases continuously as the temperature increases; (c) from 5 to 30°C where a new plateau is observed, with the discharge current remaining nearly constant (or decreasing slightly); (d) from 30 to 100°C where a higher intensity peak is observed.

The detailed analysis of these different regions was carried out systematically using the technique of thermal windowing (or thermal cleaning). This technique allows the isolation of the individual components of the complex TSDC global spectrum. The analysis of these components enables us to determine the thermokinetic parameters associated with the corresponding relaxation processes. In the following sections

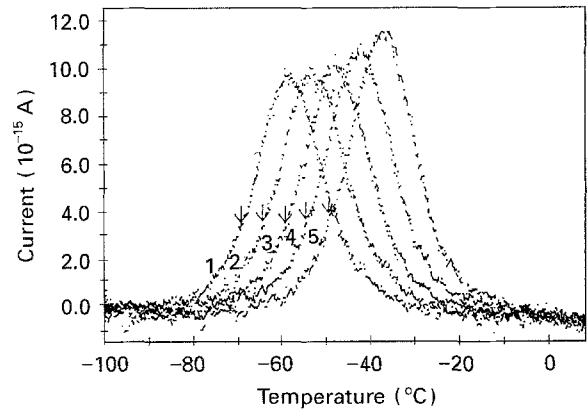


Figure 5 Thermally cleaned components of the lower temperature broad relaxation. The window width is 3°C and the polarization temperatures are: 1, -70°C ; 2, -65°C ; 3, -60°C ; 4, -55°C ; 5, -50°C .

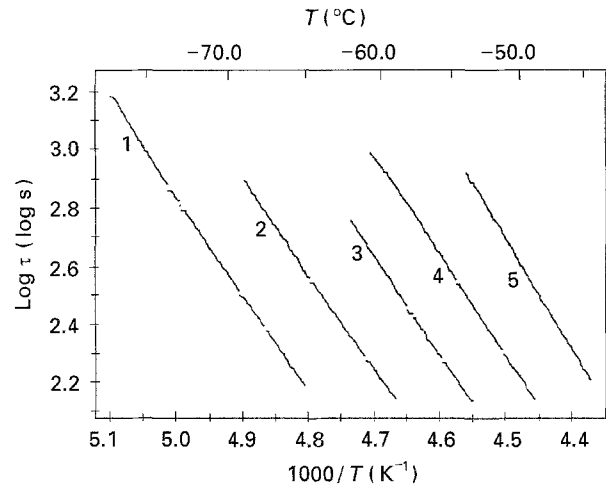


Figure 6 Arrhenius plots ($\log \tau$ versus $1/T$) for the thermally cleaned components shown in Fig. 5. The numbers indicate the correspondence between the Arrhenius lines and the peaks in Fig. 5.

the results obtained from this systematic study are reported.

3.1. The region from -100 to -50°C

Results of some of the thermal windowing experiments performed in this temperature region are shown in Fig. 5. The analysis of the different peaks allows us to draw the corresponding Arrhenius plots of $\log \tau$ versus $1/T$ (Fig. 6) and to determine the corresponding activation parameters. The relaxation time, τ , is calculated using the equation

$$\tau(T) = \frac{\int_t^\infty J(T) dt}{J(T)} \quad (1)$$

where $J(T)$ is the measured current intensity at temperature, T (readers who are not familiar with the TSDC technique and data treatment can find useful information about this subject elsewhere [13]).

From Fig. 6 we conclude that these relaxation processes show an Arrhenius behaviour. The fact that the Arrhenius lines are parallel to each other is an indication that the activation enthalpy is the same for all the individual components of the global TSDC spectrum

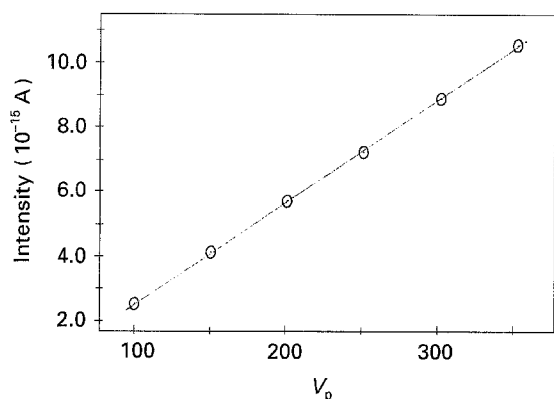


Figure 7 Maximum intensity, I_m , versus polarization voltage, V_p , for a thermally cleaned component ($T_p = -55^\circ\text{C}$) of the lower temperature broad relaxation.

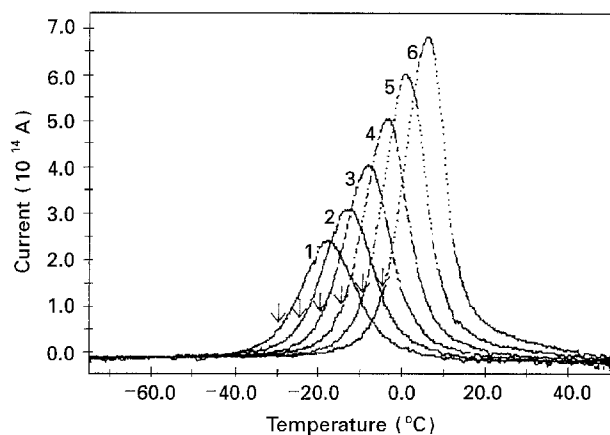


Figure 8 Thermally cleaned components in the region from -50 to 5°C . The window width is 3°C and the polarization temperatures are: 1, -30°C ; 2, -25°C ; 3, -20°C ; 4, -15°C ; 5, -10°C ; 6, -5°C .

(the calculated value is $\Delta H^\ddagger = 60\text{--}65 \text{ kJ mol}^{-1}$). On the other hand, the calculated value for the activation entropy is negligibly small (less than one entropy unit). These values of the activation parameters suggest that we are dealing with local dipolar motions which probably arise from internal rotation of polar lateral groups linked to the main chain of the polymeric materials which compose the cork cellular walls. In fact, suberin and cellulose, which constitute the walls of the cork cells [3, 14], have hydroxy and methoxy side groups which can be responsible for the observed relaxations. The dipolar nature of these molecular motions seems, on the other hand, to be confirmed by the fact that the intensity (and the area) of the discharge peaks in this temperature range show a linear dependence on the polarization voltage as shown in Fig. 7.

3.2. The region from -50 to 5°C

Fig. 8 shows the thermally cleaned components of the global spectrum in this temperature range. As expected from the global spectrum shown in Fig. 4, we observe that the intensity of the relaxation peaks increases as the polarization temperature increases. The $\log \tau$ versus $1/T$ lines corresponding to the peaks shown in Fig. 8 are presented in Fig. 9 and it is apparent that they show an Arrhenius behaviour.

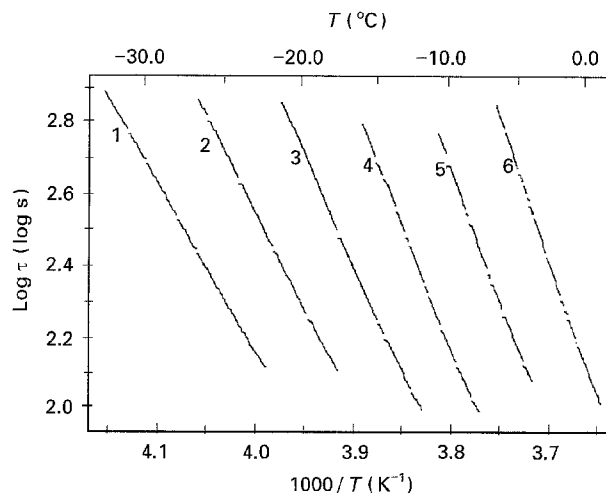


Figure 9 Arrhenius plots ($\log \tau$ versus $1/T$) for the thermally cleaned components shown in Fig. 8. The numbers indicate the correspondence between the Arrhenius lines and the peaks shown in Fig. 8.

TABLE I Activation parameters and temperature of maximum intensity, T_m , for different thermally cleaned components obtained at different polarization temperatures, T_p .

T_p ($^\circ\text{C}$)	T_m ($^\circ\text{C}$)	ΔH^\ddagger (kJ mol^{-1})	ΔS^\ddagger ($\text{J K}^{-1} \text{ mol}^{-1}$)	ΔG^\ddagger (kJ mol^{-1})
-40.0	-27.9	74.0	23.5	68.5
-35.0	-22.4	79.5	39.9	70.1
-30.0	-18.1	89.5	73.1	71.7
-25.0	-13.3	100.9	111.1	73.3
-20.0	-8.8	114.6	157.4	74.8
-15.0	-4.4	128.9	204.2	76.1
-10.0	-0.1	137.9	229.2	77.6
-5.0	4.7	149.5	262.8	79.0
0.0	9.1	163.4	303.2	80.6
5.0	13.9	167.1	307.6	81.5
10.0	18.6	169.5	306.3	82.8
15.0	23.6	156.1	247.7	84.7
20.0	28.9	142.2	188.9	86.8
25.0	34.9	128.8	132.5	89.3
30.0	48.8	119.4	95.2	90.5
30.0	51.4	116.0	81.5	91.2

The Eyring thermokinetic parameters associated with these Arrhenius plots are presented in the upper part of Table I. It can be seen that the activation enthalpies, ΔH^\ddagger , and the activation entropies, ΔS^\ddagger , show a concomitant increase as T_p increases. This is associated with the fact that a linear relationship is observed between the slopes and the intercepts of the different Arrhenius lines (compensation line) and, as a consequence, these lines converge to a single point (compensation point). The compensation point observed for the thermally cleaned individual relaxation processes in this temperature range is shown in Fig. 10 (compensation point on the right-hand side of the figure) and its coordinates are $T_c = 37.6^\circ\text{C}$ and $\log_{10} \tau_c = -1.62$ ($\tau_c = 0.055 \text{ s}$). From Table I it can also be seen that the Gibbs activation energy, ΔG^\ddagger , is a slightly increasing function of T_p .

The α process or glass transition relaxation of synthetic polymers is characterized by a compensation behaviour similar to that reported above. This behaviour

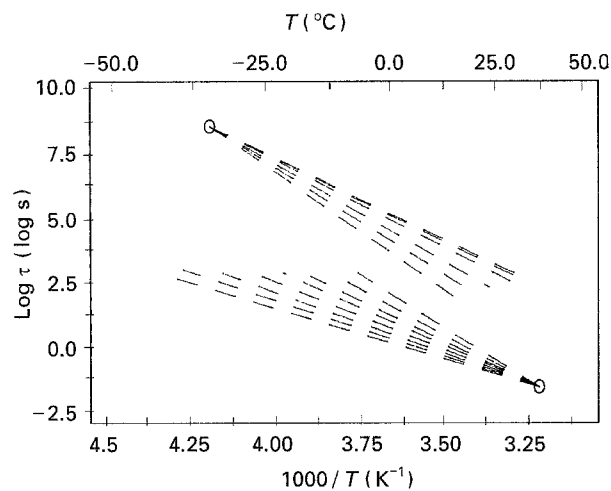


Figure 10 The compensation behaviour observed around the glass transition. The compensation point on the right-hand side corresponds to the behaviour displayed by the Arrhenius lines shown in Fig. 9 and is a characteristic of the glass transition relaxation. The compensation point on the left-hand side of the figure corresponds to the components shown in Fig. 11 and seems, as argued in the text, to be a consequence of the partial overlap of two different relaxation processes.

is considered to arise from the cooperative nature of the motions occurring at T_g which are usually ascribed to the relaxation of entities with variable dimensions. This suggests that the compensation behaviour observed in the TSDC spectrum of cork in this temperature region corresponds to a glass-transition-like process. The component which shows a maximum activation enthalpy is located in the temperature axis at $T_m = 18^\circ\text{C}$ (see Table I). Thus, it seems reasonable to consider this temperature as the glass-transition-like temperature of cork: $T_g = 18^\circ\text{C}$. The motions involved in this relaxation process seem, on the other hand, to have a dipolar nature because the discharge intensity also shows a linear variation with the polarization voltage.

3.3. The region from 5–30°C

The individual relaxation components obtained in this temperature range by the technique of thermal windowing are shown in Fig. 11 and it is apparent that the intensity of the different windows is nearly constant. In this case, contrasting with the glass transition region, we observe a decrease of the activation enthalpy and entropy with increasing polarization temperature (see lower part of Table I). The Gibbs activation energy, on the other hand, increases with increasing T_p . The results could lead us to the conclusion that we are in the presence of a compensation point with a sign which is opposite to that observed in the temperature range from -50 to 5°C (see Fig. 10). Otherwise stated, in the latter temperature range we obtain a set of lines which converge to a point at higher temperature, whereas between 5 and 30°C the lines converge to a point at a lower temperature. It was claimed [15]

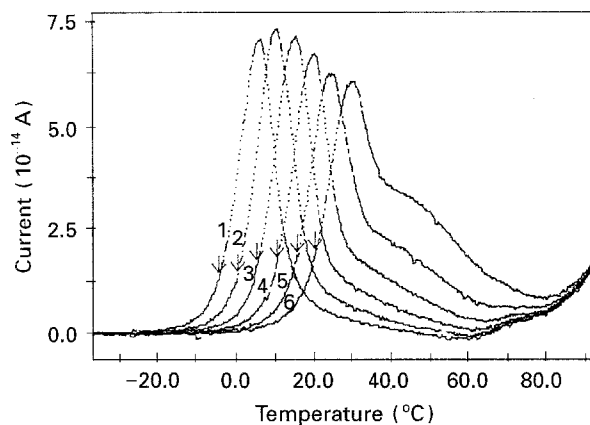


Figure 11 Thermally cleaned components in the temperature region from 5–30°C. The window width is 3°C and the polarization temperatures are: 1, -5°C ; 2, 0°C ; 3, 5°C ; 4, 10°C ; 5, 15°C ; 6, 20°C .

that the existence of a double compensation point (a “Z structure” as it is also called) is a classical behaviour across the glass transition of synthetic polymers and it was suggested that the intercept of the corresponding positive and negative compensation lines* can be used to obtain accurately the glass transition temperature, T_g , and the activation entropy and enthalpy at T_g . The glass transition temperature obtained according to this criteria is 18°C , which coincides with the value previously reported and the activation enthalpy and entropy at T_g are, respectively, 192 and $400\text{ J K}^{-1}\text{ mol}^{-1}$. Nevertheless we cannot confirm, from our previous experience on TSDC studies of polymers [12, 16], that the double compensation point (apparently shown in Fig. 10) is a genuine characteristic of the glass transition. In fact, the Z structure was not observed either in poly(vinyl acetate) [12] or in different side-chain liquid crystalline polymers that we have studied by the same technique [16, 17]. We think, on the contrary, that the Z structure which is apparent in Fig. 10 arises from the merging of two relaxation mechanisms which are partially superposed in the temperature axis of the TSC spectra. Those two mechanisms would be the glass transition relaxation and a higher temperature process which is characterized by a lower activation enthalpy and entropy but higher Gibbs activation energy. The dipolar nature of the molecular motions in this temperature region was confirmed by studies under different polarization voltages.

3.4. The region from 30–100°C

A higher intensity relaxation peak is observed in this temperature range and the analysis of its intensity dependence on the polarization voltage suggests, as for all other thermally stimulated processes studied in cork, a dipolar nature for the corresponding motions (see Fig. 12). The existence of dipolar relaxations above T_g is a very controversial subject in the polymer literature [18–22]. Different authors claim its existence

* A given compensation point is characterized by a compensation line which is the representation of the intercept versus the slope for the different Arrhenius lines in this compensation point. The existence of the compensation line indicates a concomitant variation of the enthalpy and the entropy of activation

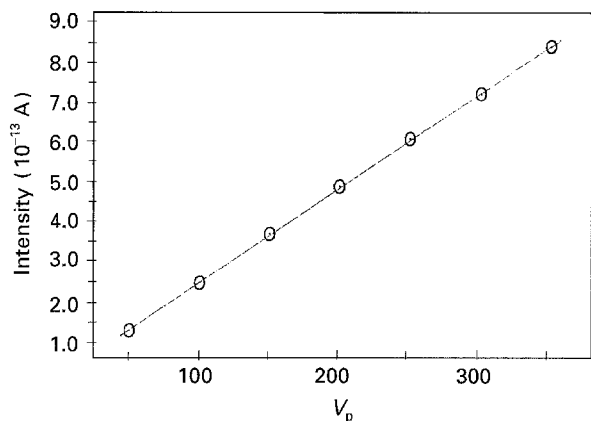


Figure 12 Maximum intensity, I_m , versus polarization voltage, V_p , for a thermally cleaned component ($T_p = -55^\circ\text{C}$) of the temperature range from 30–100°C.

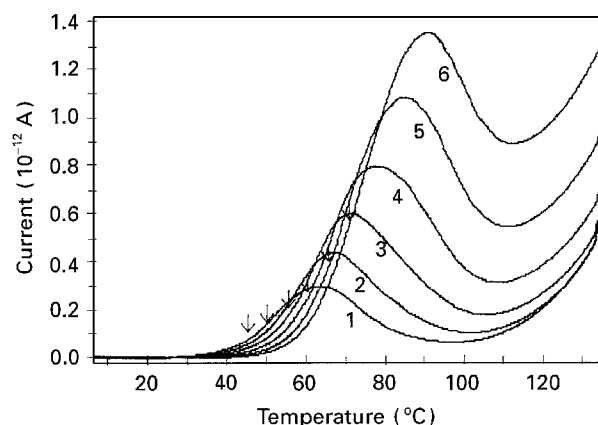


Figure 13 Thermally cleaned components of the global TSDC spectrum in the temperature region from 30–100°C. The window width is 3°C and the polarization temperatures are: 1, 45°C; 2, 50°C; 3, 55°C; 4, 60°C; 5, 65°C; 6, 70°C.

[12, 16, 22, 23] but the corresponding molecular mechanism is not yet clearly elucidated. The thermally cleaned components of this higher temperature relaxation were obtained (Fig. 13) and from their analysis it may be concluded that no compensation effect is now apparent. The activation enthalpy and entropy have thus similar values for the different windows ($\Delta H^\ddagger = 117 \text{ kJ mol}^{-1}$, $\Delta S^\ddagger = 63 \text{ J K}^{-1} \text{ mol}^{-1}$) showing that this relaxation mechanism is characterized by lower activation parameters when compared with the glass transition relaxation.

The fact that no compensation effect is observed for this discharge suggests a lower degree of cooperativity of the corresponding motions when compared with those associated with the T_g process. On the other hand, the behaviour of this discharge seems to be substantially different from the other discharges studied previously. This is illustrated in Fig. 14 where the difference $T_m - T_p$ is plotted as a function of T_p for different single relaxation components in the whole relaxation spectra. It is apparent that the behaviour in this temperature region is markedly different from the other regions, suggesting that the molecular nature of the motions involved in this relaxation is distinct from that corresponding to the other mechanisms.

Considering the values of the activation parameters which characterize this relaxation process, the temper-

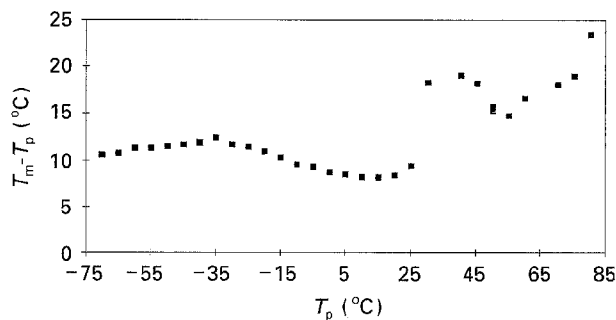


Figure 14 Plot of $T_m - T_p$ versus T_p for different single processes in the whole TSDC spectrum. The behaviour in the higher temperature region seems to be different from the other regions of the spectrum.

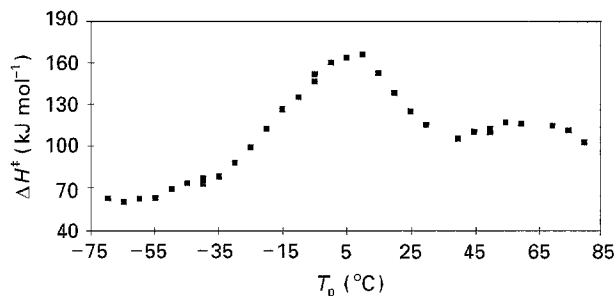


Figure 15 Activation enthalpy, ΔH^\ddagger , versus T_p for different single processes in the whole TSDC spectrum. Different regions, corresponding to different relaxation processes, are apparent in this representation.

ature region at which it occurs and the apparent non-cooperative nature of the corresponding motions, it seems reasonable to attribute this discharge to the melting process of the waxes which are one of the components of the walls of the cork cells. This attribution is strengthened by the fact that the intensity of this discharge is high when compared with that corresponding to the other processes studied before, indicating that the dipole moment relaxed in this mechanism is larger.

Finally, in Fig. 15 the activation enthalpies of the different individual components of the whole TSDC spectrum are plotted as a function of the polarization temperature. It is interesting to see that this representation clearly shows the four different regions we differentiated at the beginning of this paper on the basis of the observation of the global TSDC spectra shown in Fig. 4. Three of these regions correspond, as we have seen, to three different relaxation processes with different molecular mechanisms. The fourth region (that between 5 and 30°C) is believed to be a region of partial superposition of two different relaxation processes.

4. Conclusion

The results presented in this work show that, when submitted to static electric fields, cork exhibits a very complex pattern of polarization mechanisms. In most polymeric materials these polarization mechanisms are well separated in the temperature axis of the TSC spectra. On the other hand, in the case of cork, the relaxation processes are merged, or partially superposed, so that the global TSC spectra appears as

a continuum showing regions of different intensity (see Fig. 4). This characteristic of the TSC spectrum was also observed for poly(*n*-hexyl isocyanate) [24] which is a rigid chain rod-like polymer and is probably a consequence of the rigidity of the material at the molecular level. Cork is a very complex cellular material which is an aggregate of thin partitions and walls forming a network of cells. The cellular walls, on the other hand, are covered by complex molecular species. This pattern originates in the material a complexity and a rigidity which probably accounts for the reported characteristics of the global TSC spectra.

The detailed analysis of this complex spectra of cork was performed by a thermal windowing identification of its different components. The analysis showed that we must distinguish three different relaxation processes:

(i) One showing a compensation behaviour, indicating a high degree of cooperativity and which can be attributed to a glass-transition-like relaxation process. The existence in cork of a dipolar discharge with these characteristics allows us to suggest that cork has a glass-transition-like temperature, T_g , whose value is about 18 °C;

(ii) a lower temperature relaxation with a low activation enthalpy (63 kJ mol⁻¹) and a negligible activation entropy. The molecular motions corresponding to this relaxation are probably local motions resulting from slightly hindered internal rotations of polar groups around covalent bonds in the organic polymers which compose the walls of the cork cells;

(iii) a higher T_g mechanism with activation enthalpy of 117 kJ mol⁻¹ and activation entropy of 63 J K⁻¹ mol⁻¹. The absence of compensation in this process suggests a low degree of cooperativity and its high intensity suggests a non-local nature or, otherwise stated, a large-scale dipole motion involving eventually polymeric molecules as a whole. It is possible that this discharge is associated with the melting of the waxy substances which are present in the walls of the cork cells. Nevertheless, we must be cautious in this attribution because, as emphasized before, the molecular mechanism of these higher T_g relaxations is far from being elucidated. Studies with more microscopic techniques are needed in order to clarify this problem.

The obtained results seem to confirm the TSDC technique as a powerful method for studying dipolar motions in a very wide diversity of materials. The very high molecular complexity of cork makes it difficult to interpret in molecular terms the different discharges observed in the thermally stimulated currents spectra. Nevertheless, the results obtained constitute the first study of the properties of cork by the TSDC technique

and provide a very useful qualitative understanding of its behaviour under different electrical and thermal treatments.

Acknowledgements

This work was carried out in the context of the Unidade de Química e Física de Materiais of the Instituto de Ciência e Engenharia de Materiais-Programa Ciência. J. F. M. and N. T. C. acknowledge JNICT for their research grants. The authors thank Professors Maria Emília Rosa and M. A. Fortes for very interesting and helpful discussions about the structure and properties of cork.

References

1. J. V. NATIVIDADE, "Subcultura" (Ministério da Economia, Direcção dos Serviços Florestais e Agrícolas, Lisboa, 1950).
2. H. PEREIRA, *Wood Sci. Technol.* **22** (1988) 211.
3. P. SITTLE, *Protoplasma* **54** (1962) 555.
4. H. PEREIRA, M. E. ROSA and M. A. FORTES, *Int. Assoc. Wood Anat. Bull.* **8**(3) (1987) 213.
5. M. E. ROSA and M. A. FORTES, *Mater. Sci. Eng.* **100** (1988) 69.
6. *Idem*, *J. Mater. Sci.* **23** (1988) 35.
7. *Idem*, *ibid.* **26** (1991) 341.
8. C. M. GOMES, A. C. FERNANDES and B. S. ALMEIDA, *J. Coll. Interface Sci.* **156** (1993) 195.
9. I. M. VEIGA, A. C. FERNANDES, B. S. ALMEIDA and A. J. GROSZEK, *J. Mater. Sci. Lett.* **12** (1993) 1206.
10. M. MOURGES, M. F. HARMAND, A. LAMURE and C. LACABANNE, *J. Thermal Anal.* **40** (1993) 863.
11. A. B. DIAS, J. J. MOURA RAMOS and G. WILLIAMS, *Polymer*, **35** (1994) 1253.
12. A. B. DIAS, N. T. CORREIA, J. J. MOURA RAMOS and A. C. FERNANDES, *Polym. Int.*, **33** (1994) 293.
13. C. LACABANNE and D. CHATAIN, *J. Polym. Sci. Polym. Phys. Ed.* **11** (1973) 2315.
14. L. J. GIBSON and M. F. ASHBY, "Cellular Solids. Structure and Properties" (Pergamon Press, Oxford, 1988).
15. J. P. IBAR, *Thermochim. Acta* **192** (1991) 91.
16. J. F. MANO, J. J. MOURA RAMOS, A. C. FERNANDES and G. WILLIAMS, *Polymer* **35** (1994) 5171.
17. J. F. MANO, N. T. CORREIA, J. J. MOURA RAMOS, A. C. FERNANDES, *J. Polym. Sci. Polym. Phys. Ed.*, in press.
18. D. J. PLAZEK, *J. Polym. Sci. Polym. Phys. Ed.* **20** (1982) 1533.
19. D. J. PLAZEK and G.-F. GU, *ibid.* **20** (1982) 1551.
20. J. CHEN, L. J. FETTERS and D. J. PLAZEK, *ibid.* **20** (1982) 1565.
21. S. J. ORBON and D. J. PLAZEK, *ibid.* **20** (1982) 1575.
22. R. F. BOYER, in "Computational Modelling of Polymers", edited by J. Bicerano (Marcel Dekker, New York, 1992) pp. 1-52.
23. C. LACABANNE, P. GOYAUD and R. F. BOYER, *J. Polym. Sci. Polym. Phys. Ed.* **18** (1980) 277.
24. N. T. CORREIA, J. F. MANO and J. J. MOURA RAMOS, manuscript in preparation.

Received 15 February
and accepted 4 October 1994